Monte Carlo simulation of phase separation in K_xC_{60}

A. Touzik,* H. Hermann, and K. Wetzig
Insitute for Solid State and Materials Research Dresden, P. O. Box 270016, D-01171 Dresden, Germany
(Received 15 February 2002; published 5 August 2002)

Kinetic Monte-Carlo methods have been used to simulate phase transformations in K_xC_{60} layers. It has been found that the phase composition is controlled by a balance between the Madelung energy and the energy of the electronic-shells interaction. A density-functional calibrated tight-binding method is used to calculate electronic effects. Our calculations point out a phase separation in the fulleride layer into K-rich (K_3C_{60}) and K-depleted areas at room temperature. The two-phase system is formed as a fine mixture which is shown to be stable against aggregation. The average diameter of K_3C_{60} particles is about 20 to 40 nm and depends on the K content. This phase separation explains nanostructuring effects observed in electrochemically doped potassium fulleride layers. The size of the simulated K_3C_{60} particles correlates with the size of experimentally observed clusters. Since K_3C_{60} particles are metallic, the system considered can serve as an array of nanoelectrodes.

DOI: 10.1103/PhysRevB.66.075403 PACS number(s): 61.43.Bn, 64.75.+g, 81.30.Mh

I. INTRODUCTION

The discovery of superconductivity[1–3] in the alkali-metal-doped fullerides, in particular, K_3C_{60}, has prompted much research activity concerning their synthesis and characterization. Typically, a procedure such as the one disclosed by Holczer *et al.*,[2] is employed for substance preparation. Electrochemical methods, however, have additional benefits of the better stoichiometry control of the resulting compounds. Recently, it was found by Janda *et al.*[4] that besides K_xC_{60} phase formation, nanostructures appear in fulleride layers during electrochemical intercalation with potassium ions.

In the aforementioned work, K_xC_{60} compounds were synthesized by electrochemical reduction of thin fullerene layers in an aqueous 0.1 M KOH solution. The electrochemical method provides flexible control of composition and uniformity of potassium fulleride.[5] The process of reduction is accompanied by an irreversible intercalation of K^+ ions into the lattice of the molecular fullerene crystal. Recent results provide information that the formation of K_xC_{60} compounds under electrochemical condition is a complicated multistage process.[6] The intercalated potassium ions not only compensate excessive negative charge but also induce several kinds of structural transformations within the fullerene layer.

One of the specific effects introduced by the incorporation of potassium is concerned with the limited thermodynamical stability of K_xC_{60} phases, which strongly depends on temperature and potassium content. Potassium forms solid solutions (α-C_{60}) with C_{60} fullerenes and a number of chemical compounds. Nominally, four stoichiometric compositions of K_xC_{60} with $x=1$, 3, 4, and 6 have been indentified. Temperature-dependent x-ray photoemission (XPS) measurements as well as Raman-scattering[7] data indicate that the most stable K_xC_{60} phase at temperatures above 423K has the rock-salt structure. XPS spectra show minimal changes with increasing doping in a temperature range between 260 and 420 K. The tetrahedral to octahedral site occupancy remains unchanged at a ratio of 1:2. This behavior can be understood in terms of phase separation in K_xC_{60} systems,

$$3KC_{60} \rightarrow K_3C_{60} + 2\alpha - C_{60}. \quad (1)$$

The 298 K x-ray profile unambiguously revealed two fcc phases, with peak intensities and lattice parameters consistent with a phase separation into K_3C_{60} and α-C_{60}.[8–10] Nuclear magnetic resonance results[11] and Raman spectra[7] confirm the presence of two phases and establish their composition.

The instability of the homogeneous phase leads to significant structural transformations in the fullerene layer during the electrochemical process. It has been found that the reduction of fullerene is accompanied by an aggregation process. Clusters of potassium fulleride are formed on the surface of the fullerene layer. The molecular structure of the clusters is resolved with scanning tunneling microscopy (STM).[4] The average diameter of the clusters is about of 20 to 50 nm.

Motivated by the experimental studies of nanostructuring on the fullerene-electrolyte interface, our aim here is to gain more insight into the mechanism of this process with the help of Monte Carlo simulations. We focus on the transformations of homogeneous K_xC_{60} phases into a mixture of K-rich and essentially K-free phases. Significant difference in electrical resistivity of K_xC_{60} phases and thermodynamical instability of homogeneous phases can provide an explanation for the observed structural modifications on the surface. Experimental data on copper deposition confirm the formation of electrically conductive particles in the potassium fulleride layers.[12]

The paper is organized as follows. In Sec. II we describe our Monte Carlo simulations. It is shown that changes in Madelung energy and in electronic-shells repulsion are of primary importance to consider the redistribution of potassium ions in the fullerene layer. The results of Monte Carlo simulations are given in Sec. III. In Sec. III A we show that homogeneous K_xC_{60} phases are unstable for $x>0.1$. A fine mixture of K_3C_{60} and α-C_{60} is formed. The average size of K_3C_{60} particles is limited to 20 to 30 nm (Sec. III B). The time dependence of numerical density of K_3C_{60} particles is described in Sec. III C. Our results are summarized in Sec. IV.

TABLE I. Average Madelung constants of K_xC_{60} phases.

Phase	Lattice type	Average Madelung constant[a]
$K_{0.25}C_{60}$	simple cubic	0.528 00
$K_{0.50}C_{60}$	simple cubic	1.286 52
$K_{0.75}C_{60}$	simple cubic	2.275 57
$K_{1.00}C_{60}$	simple cubic	3.495 13
$K_{0.50}C_{60}$	fcc	1.356 08
$K_{0.75}C_{60}$	fcc	2.536 53
$K_{1.00}C_{60}$	fcc	3.931 91
$K_{1.25}C_{60}$	fcc	5.516 17
$K_{1.50}C_{60}$	fcc	7.287 22
$K_{1.75}C_{60}$	fcc	9.262 55
$K_{2.00}C_{60}$	fcc	11.455 26
$K_{2.25}C_{60}$	fcc	13.865 34
$K_{2.50}C_{60}$	fcc	16.492 79
$K_{2.75}C_{60}$	fcc	19.337 61
$K_{3.00}C_{60}$	fcc	22.399 80[b]

[a]Values for the compounds with the same composition, but different arrangement of ions can differ up to 20%.

[b]In Ref. 22 the value 22.1220 is obtained.

II. MODEL AND SIMULATION METHOD

The kinetic Monte Carlo methodology[13] has been adopted to study the redistribution of potassium ions in the C_{60} lattice. K^+ ions are considered as a three-dimensional lattice gas. It is supposed that there is no correlation between the movement of particles. Only those configurations which correspond to single-ion jump in the nearest vacancy, have a nonzero transition probability. The standard Metropolis algorithm[14] is used to generate configuration chains. The transition matrix relies on the canonical distribution of states, i.e., the probability $p_{a\to b}\propto e^{-\beta\Delta E_{ab}}$, where ΔE_{ab} depends on the local environment of an ion to be moved only. A number of effects are considered, which contribute to ΔE_{ab}.

The Madelung term V_{Mad} is calculated by using a method recently developed by Wolf.[15] This method contains no adjustable parameters as opposed to the Ewald's summation and combines high precision and computational efficiency. First, Madelung constants α_{Mad} are calculated for fcc lattices which are partially filled with potassium ions. A unit cell is chosen containing four C_{60} and up to 12 K^+ ions. Periodic boundary conditions are applied to the cell simulating bulk material. Summation is carried for systems containing n^3 cells starting with $n=10$ and finishing if the $(n+1)$ contribution was smaller than 10^{-7}, which happened in most cases at about $n=15$–20. This procedure was repeated for all unit cells having the same composition but different ion arrangement. The values obtained by averaging over all possible ion arrangements are given in Table I as a function of the population of tetrahedral and octahedral interstitials. The results in Table I are valid for uniform distribution of the negative charges on the fullerene particles. Nonuniform distributions of electrons among C_{60} particles was also considered. There, the results for different charge distributions scattered around the corresponding value for uniform distribution with deviations of less than 2%.

TABLE II. Empirical parameters for the Madelung constant expression, Eq. (2).

n	Empirical parameter a_n
1	0.1630 03
2	0.3089 28
3	0.5837 05
4	0.0447 28
5	0.5885 82

It has been found that a parabolic-type function fits the calculated data well,

$$\alpha_{Mad}=a_1n_o^2+(a_2n_t+a_3)n_o+(a_4n_t^2+a_5n_t), \qquad (2)$$

where $a_1\cdots a_5$ are empirical parameters (see Table II), n_t and n_o are the populations of the tetrahedral and octahedral interstitials, respectively. The Madelung energy change associated with one K^+ ion jump is

$$V_{Mad}(x_0',x')=k'q^2[\alpha_{Mad}(x')/a-\alpha_{Mad}(x_0')/a_0], \qquad (3)$$

where k' is Coulomb's constant in eV, x' is the local concentration of potassium near the vacancy, q is the charge on the ions, and a is the distance between neighboring ions. The quantities x' and a_0 denote the corresponding parameter values before the jump. The Madelung energy change is of the order of several eV.

The density-functional tight-binding (DFTB) method, originally described by Porezag *et al.*[16] is used to estimate the electronic-shells interaction energy $V_{el.sh.}$. It was calculated for a pair of C_{60} molecules for a series of distances which are representative for the experimental values for the C_{60} compounds. The difference between C_{60} ions and molecules can be neglected in this case due to the large number of the valence electrons per C_{60}. The DFTB data are used in our Monte-Carlo simulations as follows. The occupation number of octahedral and tetrahedral interstitials in the local environment of the K^+ ion to be moved is determined. Depending on the occupation number the actual C_{60}-C_{60} distance is selected among the experimental data for the pristine C_{60}, the K_3C_{60}, and the high-temperature KC_{60} phase. The corresponding DFTB energy is taken as $V_{el.sh.}$. The energy of the electronic shells interaction is of the order of up to several eV.

We have also considered additional effects which can contribute to the total energy. First, we used a two-step procedure to calculate the polarization energy of C_{60} molecules (ions). At the first step, radial distribution functions (RDF) for K^+ in C_{60} lattice were evaluated by means of DFTB molecular dynamics.[16] Then the RDFs were combined with results of *ab initio* data for K^+-C_{60} system. *Ab initio* density-functional calculations within the local-density approximation using a numerically generated basis set were performed for this system by Li and Tomanek.[17] The maximal value of the polarization energy is about 0.1 eV. Second, intercalation with potassium restricts rotation of C_{60} molecules (ions), and, therefore, it changes the entropy term of free energy. We estimated this contribution with a method described by Grá-

násy *et al.*[18] The effect is about 0.05 eV. This value is in agreement with the last low-temperature heat-capacity data for K_3C_{60}, presented by Allen and Hellman.[19] Third, the energy change, caused by C_{60} van der Waals interaction was estimated using Girifalko[20] empirical potential and found to be negligible.

The final Hamiltonian reads

$$H = V_{Mad} + V_{el.sh.} + V_{minor}, \tag{4}$$

where V_{Mad} is the Madelung energy, $V_{el.sh.}$ is the energy of the electronic-shells interaction, and V_{minor} corresponds to minor effects. The simulation time was about 10^6 Monte Carlo steps (MCS). One Monte Carlo step consists of N^2M and $3N^2M$ move trials for the cubic and fcc C_{60} lattices, respectively.

We suppose that the electrochemical injection of potassium ions into the fullerene layer proceeds much faster than the following relaxation processes. We consider the reaxation processes, in particular the phase separation, as the limiting stage of the total evolution. We focus on the process of potassium ion redistribution inside the C_{60} lattice. The initial state is a random uniform distribution of potassium in the fulleride layer with fixed mean potassium content. Systems with nonuniform (gradient) initial distribution are also considered.

Phase boundaries in the K_xC_{60} layer are determined as follows. The potassium concentration is calculated with respect to the nearest environment for each interstitial site of the C_{60} lattice. If the local concentration exceeds 2.6, the site is marked as ''K rich.'' If it is lower than 0.4, the site is marked as ''K free.'' Neighboring ''K-rich'' or ''K-free'' sites belong to the same particle of K-rich or K-free phase, respectively. Once phase boundaries have been determined, the evolution of a particle size or a number density is calculated in a straightforward way.

We consider a face-centered cubic (fcc) fixed-node lattice of C_{60} molecules (ions). There is a lattice of $N\times N\times M$ cells with periodic boundary conditions in the x and y directions. Along the z axis the system is limited by two surfaces (see Fig. 1). Throughout most of our calculations, systems of typical size $N=M=64$ are considered. No influence of unit size on the output parameters was found in a number of runs with $N=128$, $M=64$ and $N=64$, $M=128$. There are two possible ways, how K^+ ions can be distributed in the C_{60} fcc lattice. First, K^+ ions occupy only octahedral interstitials and form the rock-salt type (simple cubic) lattice. Second, K^+ ions occupy both octahedral and tetrahedral interstitials (fcc lattice).

III. RESULTS AND DISCUSSIONS

A. General kinetic evolution

Our Monte Carlo calculations clearly show phase separation in the K_xC_{60} layers, where x ranges from 0.1 to 3. Three characteristic cases with different potassium contents are taken to illustrate the results: $K_{0.125}C_{60}$ (low), $K_{0.25}C_{60}$ (medium), and $K_{0.5}C_{60}$ (high). Figure 1 shows a typical distribution of potassium in the fulleride layer at high potassium content. ''K-rich'' (K_3C_{60}) and ''K-free'' (α-C_{60}) phases occupy more than 90% of the layer volume. Two phases coexist as a mixture of fine particles. The average size of the K_3C_{60} particles is about tens of nanometers.

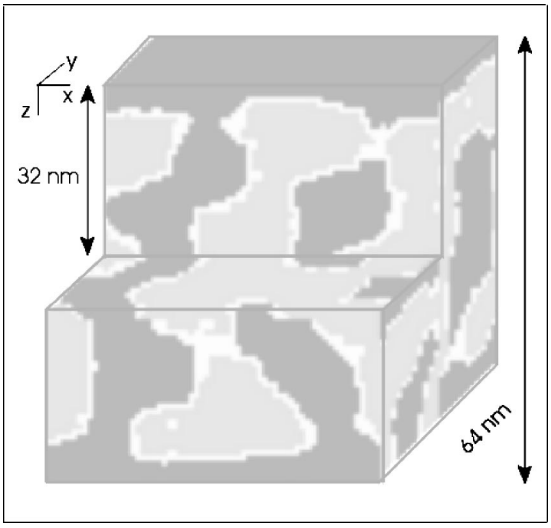

FIG. 1. Cross section of a $K_{0.5}C_{60}$ layer after decomposition into K_3C_{60} clusters (light gray) and regions depleted with respect to K^+ ions (dark gray).

Figure 2 shows the change of the volume fraction (n_v) of the K_3C_{60} phase as a function of time. After approximately 10^6 MC steps the volume fraction approaches a limit. Limit values of the volume fraction are substantially lower than expected. It means that a fine mixture of K_3C_{60} and α-C_{60} phases remains stable over a long time. The mean particle size and its dependence on the potassium content in the layer will be discussed below.

The following empirical function fits well the evolution of the K_3C_{60} volume fraction:

$$n_{vol} = n_1 + n_2, \quad n_i = a_i t/(1+b_i t), \quad i=1,2, \tag{5}$$

where $b_1 \ll b_2$. The terms in Eq. (5) correspond to two types of processes during the phase separation. This two-stage re-

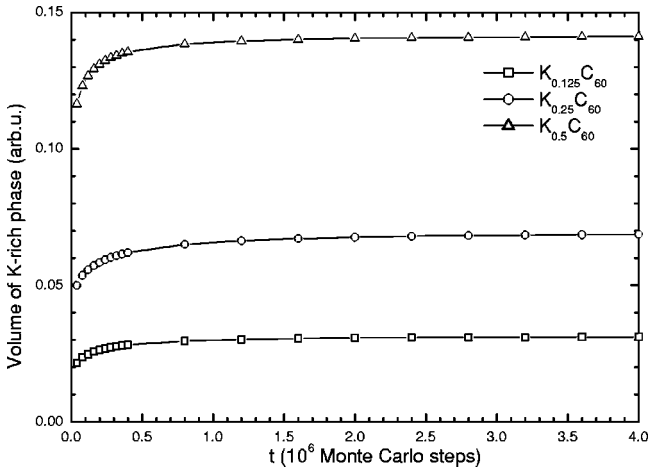

FIG. 2. Volume part of K-rich phase for three different K_xC_{60} stoichiometries.

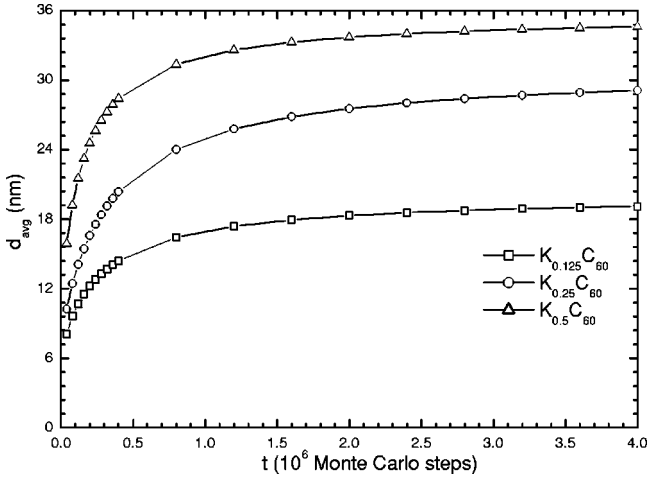

FIG. 3. Time dependence of the average size of K_3C_{60} particles for three different K_xC_{60} stoichiometries.

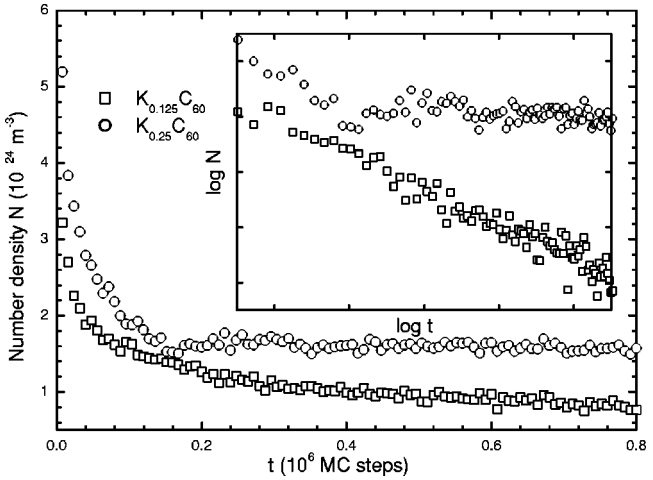

FIG. 4. Time dependence of the number density of $K_{0.125}C_{60}$ and $K_{0.25}C_{60}$ stoichiometries.

distribution of potassium ions is interpreted in terms of growth and coarsening. the first 10^4 MCS correspond to a ''growth+coarsening'' regime. After that the process can be considered as a pure coarsening.

It has been found that the primary mechanism of coarsening of the K_3C_{60} particles depends on the potassium content in the layer. At low concentrations, growth or dissolution of K_3C_{60} particles proceeds through the diffusion of single K^+ ions. At high potassium content, coalescence of K_3C_{60} particles becomes more important.

The ''K-rich'' and ''K-free'' phases have substantially different electrical properties. The resistivity of the K_3C_{60} and α-C_{60} phase at room temperature is 4.94 mΩ cm and $\sim 5 \times 10^5$ mΩ cm, respectively. This means that the phase separation will strongly affect electrochemical processes. Recent experiments on the growth of metal films on K_xC_{60} substrates provide an indirect evidence of inhomogeneous distribution of particles with different electrical conductivity inside the fulleride layer.[12]

B. Particle size

The time dependence of the average size of K_3C_{60} particles is presented in Fig. 3. The particles exhibit stability of their dimensions for a long simulation time. Typical values for the particle size are in the range of 20 to 40 nm. The distribution of the particle size is far from uniformity. We estimate maximal size of particles from 50 to 60 nm. Small grains of K_3C_{60} phase form during the first few Monte Carlo steps. The next stage is characterized by growth of K_3C_{60} particles as well as redistribution of potassium ions among them. The average particle size reaches about 70% of its final value at the end of this stage. The late stage is a migration of potassium ions from small K_3C_{60} particles to big ones.

We also investigated the influence of the V_{minor} Hamiltonian term on the K_3C_{60} particle size. Polarization energy and enthropy effects have the most considerable effect on the dynamics of the phase separation. The limiting values of the particle size remain approximately the same. The potassium content in the fulleride layer is the main factor affecting the average size of particles. The difference in particle size amounts to a factor 2 between the $K_{0.125}C_{60}$ and the $K_{0.5}C_{60}$ systems.

There is a good correlation between the diameter of K_3C_{60} particles calculated here, and the diameter of the appropriate clusters on the surface measured in STM experiments. We suppose that the instability of homogeneous potassium fulleride phase is the reason for the nanostructure formation on the surface. Therefore variation of the composition of the fulleride layer can be used to control structural modifications on the surface. In particular, mean size and density of the clusters will be affected by the amount of charge and, accordingly, the number of counterions, injected into the layer.

C. Number density of particles

In order to compare our results with predictions of phenomenological macroscopic theories the number density of particles was calculated. The Lifshitz-Slyozov-Wagner (LSW) theory of coarsening concerns the time evolution of the size distribution of a dilute system of particles that evolve by diffusional mass transfer.[21] According to the LSW model,

$$\overline{R^3} - \overline{R_0^3} = \alpha_{LSW} t, \tag{6a}$$

should apply, when steady-state distribution of particle sizes has been achieved, where $\overline{R}$ is the average particle size, $\overline{R_0}$ is the initial average particle size, α_{LSW} is a constant, and t is the time. Accordingly, the number density N is expressed as

$$N = N_0/[1 + (\alpha_{LSW}/\overline{R_0^3})t], \quad N \propto t^{-1} \quad \text{if } t \to \infty. \tag{6b}$$

The calculated densities of K_3C_{60} particles for $K_{0.125}C_{60}$ and $K_{0.25}C_{60}$ are presented as a function of time in Fig. 4. It is hard to distinguish individual K_3C_{60} particles for systems with a higher potassium content, because particles are in close contact with each other. On the inset the same data are presented on a logarithmic scale.

The particle density is a linear function on the logarithmic scale for the layers with a small as well as with a medium potassium content, i.e., $N \propto t^{-n}$. The growth exponents n are considerably lower than the value predicted by the LSW model. The values of n depend on the composition of the layer and reside between 0.30 and 0.45. A number of reasons exist, why the coarsening of the K_3C_{60} particles does not obey the LSW law. The LSW model assumes, in particular, a diffusional control of the particle growth. In our case, diffusion is, probably, not essential during the limiting stage of the whole process. Taking into account that there are a limited number of ways to implement movement of potassium ions in the fullerene lattice, ion rearrangement at the interface may be responsible for slowing down the growth. As the potassium content in the layer is enhanced, the second region on the particle density curve appears (Fig. 4, inset). The density remains constant after some point, and K_3C_{60} and α-C_{60} coexist as a fine mixture.

The particle density depends on the potassium content in the layer. The reason is, probably, that two different mechanisms of the particle growth are active. Experimentally, the potassium contents in the layer and, accordingly, size and density of fulleride clusters can be adjusted by the potential sweep rate and other parameters of the electrochemical process.

IV. SUMMARY AND CONCLUDING REMARKS

Phase separation in K_xC_{60} systems is shown to be an essential effect in understanding of nanostructuring phenomena under electrochemical conditions. The structural modifications observed experimentally on the surface of potassium doped fullerene layers come out as a result of nanometer scale fluctuations of the electrical conductivity, induced by the formation of metallic K_3C_{60} nanoparticles. The kinetic Monte Carlo method is adopted to investigate the processes of phase separation in potassium fulleride layers. It has shown that local changes of the Madelung energy are the driving force of the phase separation. The equilibrium potassium distribution is mainly determined by a balance between electrostatic attraction and C_{60}-C_{60} electronic shells repulsion. The average size of K_3C_{60} is found to be limited to 20 to 40 nm. The maximal size of the particles is about 50 to 60 nm. The calculated size of the K_3C_{60} nanoparticles inside the potassium fulleride layer correlates with the size of the clusters on the layer surface observed by STM. It is predicted that the size and the size distribution of the clusters can be controlled by the amount of charge injected electrochemically into the fullerene layer. Since there is a large difference between the electrical conductivity of the K_3C_{60} particles and K-depleted zones, the systems discussed can be used as random arrays of nanoelectrodes.

ACKNOWLEDGMENTS

This work was supported by the Deutsche Forschungsgemeinschaft (DFG focus program ''Foundations of electrochemical nanotechnology'').

*Also at Research Institute for Physical and Chemical Problems, Minsk, Belarus.

[1] A. Hebard, M. Rosseinsky, R. Haddon, D. Murphy, S. Glarum, T. Palstra, A. Ramirez, and A. Kortan, Nature (London) **350**, 600 (1991).

[2] K. Holczer, O. Klein, S. Huang, R. Kaner, K. Fu, R. Whetten, and F. Diederich, Science **252**, 1154 (1991).

[3] M. Rosseinsky, A. Ramirez, S. Glarum, D. Murphy, R. Haddon, A. Hebard, T. Palstra, A. Kortan, S. Zahurak, and A. Makhija, Phys. Rev. Lett. **66**, 2830 (1991).

[4] P. Janda, T. Krieg, and L. Dunsch, Adv. Mater. **10**, 1434 (1998).

[5] G. Vaughan, M. Barral, T. Pagnier, and Y. Chabre, Synth. Met. **77**, 7 (1996).

[6] P. Janda, T. Krieg, P. Georgi, M. Gembicka, S. Oswald, and N. Mattern, *Elektrochemische Verfahren für neue Technologien, Monographie/GDCh* (2001).

[7] J. Winter and H. Kuzmany, Solid State Commun. **84**, 935 (1992).

[8] Q. Zhu, O. Zhou, N. Bykovetz, J. Fischer, A. McGhie, W. Romanow, C. Lin, R. Strongin, M. Cichy, and A. B. Smith III, Phys. Rev. B **47**, 13 948 (1993).

[9] G. Faigel, *et al.*, Phys. Rev. B **52**, 3199 (1995).

[10] D. Poirier, T. Ohno, G. Kroll, P. Benning, F. Stepniak, J. Weaver, L. Chibante, and R. Smalley, Phys. Rev. B **47**, 9870 (1993).

[11] R. Tycko, G. Dabbagh, M. Rosseinsky, D. Murphy, R. Fleming, A. Ramirez, and J. Tully, Science **253**, 884 (1991).

[12] A. Touzik, H. Hermann, P. Janda, L. Dunsch, and K. Wetzig, Europhys. Lett. (to be published).

[13] A. Levi and M. Kotrla, J. Phys.: Condens. Matter **9**, 299 (1997).

[14] N. Metropolis, A. Rosenbluth, and E. Teller, J. Phys. Chem. **21**, 1087 (1953).

[15] D. Wolf, P. Keblinski, S. Phillpot, and J. Eggebrecht, J. Chem. Phys. **110**, 8254 (1999).

[16] D. Porezag, T. Frauenheim, T. Köhler, G. Seifert, and R. Kaschner, Phys. Rev. B **51**, 12 947 (1995).

[17] Y. Li and D. Tomanek, Chem. Phys. Lett. **221**, 453 (1994).

[18] L. Gránásy, S. Pekker, and L. Forró, Phys. Rev. B **53**, 5059 (1996).

[19] K. Allen and F. Hellman, Phys. Rev. B **60**, 11 765 (1999).

[20] L. Girifalko, J. Phys. Chem. **96**, 858 (1992).

[21] I. Lifshitz and V. Slyozov, J. Phys. Chem. Solids **19**, 35 (1961).

[22] Y. Wang, D. Tomanek, G. Bertsch, and R. Ruoff, Phys. Rev. B **47**, 6711 (1993).